

Post-Newtonian effects in compact binaries with a dark matter spike: A Lagrangian approach

Diego Montalvo,^{1,2,*} Adam Smith-Orlik,^{3,†} Saeed Rastgoo,^{4,5,6,‡}
Laura Sagunski,^{7,§} Niklas Becker,^{7,¶} and Hazkeel Khan^{3,**}

¹*Canadian Institute for Theoretical Astrophysics, University of Toronto,
60 St. George Street, Toronto, ON M5S 3H8, Canada*

²*Department of Physics, University of Toronto,
60 St. George Street, Toronto, ON M5S 1A7, Canada*

³*Department of Physics and Astronomy, York University
4700 Keele Street, Toronto, Ontario M3J 1P3 Canada*

⁴*Department of Physics, University of Alberta,
Edmonton, Alberta T6G 2G1, Canada*

⁵*Department of Mathematical and Statistical Sciences,
University of Alberta, Edmonton, Alberta T6G 2G1, Canada*

⁶*Theoretical Physics Institute, University of Alberta,
Edmonton, Alberta T6G 2G1, Canada*

⁷*Institute for Theoretical Physics, Goethe University, 60438 Frankfurt am Main, Germany*
(Dated: January 12, 2024)

We present a simple but powerful Lagrangian method that can be used to study the post-Newtonian evolution of a compact binary system with environment, including a dark matter spike, around it, and obtain the resulting gravitational wave emission. This formalism allows one to incorporate post-Newtonian effects up to any desired known order, as well as any other environmental effect around the binary, as long as their dissipation power or force formulae are known. In particular, in this work, we employ this method to study a black hole-black hole binary system of mass ratio 10^5 , by including post-Newtonian effects of order 1PN and 2.5PN as well as the effect of relativistic dynamical friction. We obtain the modified orbits and the corresponding modified gravitational waveform. Finally, we contrast these modifications against the LISA sensitivity curve in frequency space and show that this observatory can detect the associated signals.

I. INTRODUCTION

The first direct detection of gravitational waves (GWs) by the LIGO/Virgo collaboration has opened up a new window into the universe [1]. Mergers of compact binary objects, such as black holes and neutron stars, provide unprecedented precision tests of general relativity and matter at its highest densities. There are also plans for space-based GW

* montalvo@cita.utoronto.ca

† asorlik@yorku.ca

‡ srastgoo@ualberta.ca

§ sagunski@itp.uni-frankfurt.de

¶ nbecker@itp.uni-frankfurt.de

** hazkeelk@my.yorku.ca

observatories such as The Laser Interferometer Space Observatory (LISA) [2], Taiji [3] and TianQuin [4]. These will be able to observe GWs at lower frequencies and thus, to observe mergers of massive binary black holes and intermediate and extreme mass ratio inspirals (EMRIs/IMRIs). These systems are considered to be a rich source of signatures associated to various new and fundamental physics phenomena [5–11], and in particular dark matter (DM). The standard cosmological Λ CDM model predicts the existence of such dark matter, a cold, collisionless massive particle, which has so far eluded our direct detection efforts [12]. Utilizing this new window into the universe, GW probes of dark matter have been gaining traction in recent years [13].

When Intermediate Mass Black Holes (IMBHs) undergo adiabatic growth within DM halos, overdensities of DM, so-called DM *spikes*, can form [14, 15]. The presence of these DM spikes can affect an inspiraling object as part of an IMRI. This has first been explored in [16, 17], where the DM spike interacts with the compact object through dynamical friction. This results in a faster inspiral compared to an inspiral in a vacuum and would be observable as a *dephasing* of the GW signal, possibly detectable by LISA [18, 19].

Additional effects of these DM spikes have been explored in consecutive works, such as the effects of accretion of the DM spike [20, 21], eccentric orbits inside these DM spikes [22–25], periastron precession [26], the halo feedback mechanism [19, 27], relativistic corrections to dynamical friction and spike distribution [28], and DM spikes around primordial black holes [29]. These works all explore different effects, that need to be combined in the end, as precise waveforms are needed to find them in the LISA data [30].

In this work, we will present a general Lagrangian framework that can easily incorporate post-Newtonian (PN) corrections, dark matter dynamical friction, accretion, and any other orbital or environmental effect in a compact binary system with environment, as long as the mathematical formula of the aforementioned effects and corrections are known in the form of a dissipative power or a force. These effects are then formulated as generalized forces, and the Euler-Lagrange equations of motion yield the modified orbits, from which the waveform of the gravitational waves emitted by the binary system can be derived. Thus this framework is different from other approaches that assume the quasi-adiabatic inspiral in their computations.

The structure of this paper is as follows. In Sec. II, we present the system we are considering for applying our Lagrangian formulation to and describe the model used for the DM spike profile. In Sec. III, we present the main proposal of the paper, namely the introduction of a Lagrangian formulation which can incorporate all the PN corrections up to any order, as well as other effects such as dynamical friction due to DM and mass accretion by the binary system. Sec. IV is dedicated to studying the system detailed in Sec. II using the Lagrangian formalism of Sec. IV. There, we compute the orbits, from which we derive the waveform of the GWs emitted by the compact binary system surrounded by a spike. We also compare the results with no-DM and no-PN cases, and by an analysis in the frequency space, show that these modifications to the GWs can be observed by LISA. Finally, in Sec. V we summarize our work and make some concluding remarks about the potential further applications of the Lagrangian framework we present in this paper.

II. DARK MATTER HALO

A. Spike profile

We consider a Schwarzschild black hole (BH) with mass m_1 that grows adiabatically and forms a surrounding DM spike $\rho_{\text{DM}}(r)$ that concentrates DM from an initially Navarro-Frenk-White (NFW) profile [31]. A second smaller compact object of mass $m_2 \ll m_1$ is on an approximately Keplerian orbit around the BH and experiences dissipative forces from gravitational wave emission and dynamical friction from the DM halo, which cause an inspiral due to the loss of orbital energy.

During the adiabatic growth of the central BH a DM halo can contract and form a spike, resulting in large DM densities close to the BH horizon. The DM density profile describing such a spike has been derived first in a semi-relativistic Newtonian manner [14], and later in a fully relativistic way [15]. The fully relativistic model predicts that the DM density vanishes at $2R_s$ compared to $4R_s$ predicted by the semi-relativistic treatment, where R_s is the Schwarzschild radius of the BH. Further, the central densities of the relativistic DM spike can be significantly higher compared with the semi-relativistic case. Higher DM densities can have a significant impact on the rate of inspiral and hence the gravitational wave signal, therefore we elect to use the fully relativistic model for our DM spike.

To model a relativistic DM density spike we follow the effective scaling function, Eq. (7) in [28], given as,

$$\rho_{\text{DM}}(r) = \bar{\rho} 10^\delta \left(\frac{\rho_0}{0.3 \text{GeV}/\text{cm}^3} \right)^\alpha \left(\frac{m_1}{10^6 M_\odot} \right)^\beta \left(\frac{a}{20 \text{kpc}} \right)^\gamma, \quad (2.1)$$

with

$$\bar{\rho} = A \left(1 - \frac{4}{\tilde{x}} \right)^w \left(\frac{4.17 \times 10^{11}}{\tilde{x}} \right)^q, \quad (2.2)$$

where $\alpha, \beta, \gamma, \delta$, are the relativistic NFW parameters generated by comparing to numerically generated curves; A, w , and q are fit parameters found by fitting to a reference curve with the scale parameters $(\rho_0, M_{\text{BH}}, a) = (0.3 \text{GeV}/\text{cm}^3, 10^6 M_\odot, 20 \text{kpc})$; and $\tilde{x} = r/m_1$ (see Table 1 in Ref. [28])¹.

For the inspiral process, the DM halo is assumed to be static. This assumption ignores the effects of dynamical friction on the DM halo itself² which can be significant for binary systems with mass ratios less than 10^5 as shown in Ref. [27]. Nevertheless, in this work, we first want to check the consistency of the Lagrangian formulation by exploring the effects of post-Newtonian correction terms.

In the presence of a DM spike, the additional dissipative forces will speed up the inspiral, which is potentially observable in the GW signal. Therefore, it should in principle be possible to map out the spike density. Using a similar analysis to [29] matched-filtering searches are powerful tools for GW detections and parameter inference. It is, however, necessary to utilize suitable GW templates, which by taking into account a broader class of physical effects such as a relativistic DM spike or orbital evolution beyond the Newtonian regime, could improve the possibilities of potential detections. We consider the evolution of the binary system slightly before GW emission enters the lower end of the detector's band. For our binary

¹ Note that $\rho_{\text{DM}}(r)$ is a valid fit when $r \ll a$ and $0.01 \text{kpc} \leq a$.

² This process is known as halo feedback.

mass considerations, this coincides with regions of high density from the DM spike at a distance from the central BH of about a hundred times the innermost stable circular orbit, r_{ISCO} , defined as

$$r_{\text{ISCO}} = 3R_s. \quad (2.3)$$

B. System parameters

To avoid the effect of halo feedback, we focus our study on a central mass of $10^6 M_\odot$ ³ with a $10M_\odot$ companion. This yields a mass ratio of 10^5 , which ensures the DM halo's binding energy is greater than energy dissipation by dynamical friction, ensuring the validity of the static halo approximation [27]. To emphasize the sensitivity of the inspiral due to the DM density, we present three DM spikes in Sec. IV with varying scale densities, ρ_0 , i.e. $\rho_0 = (0.1, 0.3, 0.5)$ GeV/cm³.⁴ For simplicity, we match the scale radius to the reference value, i.e. $a = 20$ kpc. Moreover, we assume a distance of 1 Mpc from the Earth to the binary, and a total inspiral distance for the companion to be from $100r_{\text{ISCO}}$ to $3r_{\text{ISCO}}$, which is sufficient to show the effects of PN corrections, DM friction, while also being inside the range of LISA's sensitivity band.

III. LAGRANGIAN FORMULATION AND EQUATIONS OF MOTION

To incorporate post-Newtonian (PN) corrections and DM effects in our model to be able to compute the orbits with these corrections taken into account, we use the Lagrangian formulation and encapsulate both PN and DM effects as generalized forces in this method. To see this more clearly, consider a system that is under both b conservative forces $\tilde{\mathbf{F}}^{(b)}$ and l non-conservative forces $\mathbf{F}^{(l)}$. The Lagrangian of the system can still be written as

$$L = T - V \quad (3.1)$$

where T is the kinetic energy of the system and V is the potential energy associated to the conservative forces $\tilde{\mathbf{F}}^{(b)}$. However, using the d'Alembert principle, the Euler-Lagrange (E-L) equations of motion can be written as⁵

$$\frac{d}{dt} \left(\frac{\partial L}{\partial \dot{q}^i} \right) - \frac{\partial L}{\partial q^i} = \sum_l Q_i^{(l)} \quad (3.2)$$

where $Q_i^{(l)}$ represent generalized forces corresponding to non-conservative forces $\mathbf{F}^{(l)}$, i.e.,

$$Q_j^{(l)} = \mathbf{F}^{(l)} \cdot \frac{\partial \mathbf{r}}{\partial q^j} = F_i^{(l)} \frac{\partial x^i}{\partial q^j}. \quad (3.3)$$

Here \mathbf{r} is the Cartesian position vector of the object (or subsystem), and q^j are its generalized coordinates, where in 3D $j = 1, 2, 3$. We can adopt q^j to spherical coordinates such that $q^1 = r$, $q^2 = \theta$, $q^3 = \phi$, and thus

$$\mathbf{r} = (x^1, x^2, x^3) = (x, y, z) = (r \cos(\phi) \sin(\theta), r \sin(\phi) \sin(\theta), r \cos(\theta)). \quad (3.4)$$

³ Which matches with the scale M_{BH} in Eq. (2.1)

⁴ Corresponding to the three DM scale densities tested in Ref. [28].

⁵ We use Einstein's summation notation and the indices are raised and lowered with the flat Euclidean metric $\delta_{ij} = \text{dig}(1, 1, 1)$.

If the motion is restricted to a 2D plane, for example, in the case of a Keplerian orbit of a planet with $\theta = \frac{\pi}{2}$, then we can effectively work with just two coordinates $q^1 = r$, $q^2 = \phi$, and thus

$$\mathbf{r} = (x^1, x^2) = (x, y) = (r \cos(\phi), r \sin(\phi)). \quad (3.5)$$

For such a 2D system with l non-conservative forces, Eq. (3.2) becomes

$$\frac{d}{dt} \left(\frac{\partial L}{\partial \dot{r}} \right) - \frac{\partial L}{\partial r} = \sum_l Q_r^{(l)}, \quad (3.6)$$

$$\frac{d}{dt} \left(\frac{\partial L}{\partial \dot{\phi}} \right) - \frac{\partial L}{\partial \phi} = \sum_l Q_\phi^{(l)}. \quad (3.7)$$

As mentioned above, in our model we will be dealing with both the PN corrections and the so-called dynamical friction effects. The latter stems from the interaction of the orbiting object (with lower mass) with its local DM environment and has nothing to do with friction in an electromagnetic sense.

In what follows, we will conveniently add the conservative Newtonian potential to the Lagrangian itself, while the PN and the dynamical friction terms, which are velocity-dependent, will be added to the equations of motion as generalized forces. Among the aforementioned PN terms and of particular interest is the effect of the GW radiation which is precisely equivalent to the so-called order 2.5 PN correction term [32].

A. Conservative part (Lagrangian) of the Euler-Lagrange equations

As mentioned above, in our two-body system that is surrounded by a DM spike, in the center of mass (CM) frame we can write the Lagrangian as

$$L = \frac{1}{2} \mu \dot{\mathbf{r}}^2 - V(r) \quad (3.8)$$

where $\mathbf{r} = \mathbf{r}_1 - \mathbf{r}_2$ is the relative position of the objects in which indices 1, 2 refer to the central and the rotating objects respectively, and $\dot{\mathbf{r}}^2 = \dot{r}^2 + r^2 \dot{\phi}^2$. We denote the mass of the central more massive object by m_1 and the lighter orbiting object by m_2 . Furthermore, the total mass of the two-body system is denoted by $m = m_1 + m_2$ and its reduced mass by $\mu = m_1 m_2 / m$. The potential used in the Lagrangian is the Newtonian gravitational potential energy between the two bodies,

$$V(r) = -G \frac{\mu m}{r}. \quad (3.9)$$

Both masses can potentially be time-dependent if one also considers the accretion effect by which they absorb DM from the DM spike around the central object.

B. Generalized forces

Once we have the Lagrangian, we can easily write down the left-hand side of the E-L equations (3.6)–(3.7). To write the right-hand side of these equations, we need to find the generalized forces. To do that, we assume that the corresponding usual forces themselves

have two components: One component is (anti)parallel to the relative velocity of the objects $\mathbf{v} = \mathbf{v}_1 - \mathbf{v}_2$, and the second component is (anti)parallel to $\mathbf{r} = \mathbf{r}_1 - \mathbf{r}_2$, along the line connecting the two bodies. Such a force can be written in the form

$$\mathbf{F}^{(l)} = F_r^{(l)} \hat{\mathbf{r}} + F_v^{(l)} \hat{\mathbf{v}}. \quad (3.10)$$

The generalized force corresponding to this force is

$$Q_j^{(l)} = \mathbf{F}^{(l)} \cdot \frac{\partial \mathbf{r}}{\partial q^j} = \frac{F_r^{(l)}}{r} \left(x \frac{\partial x}{\partial q^j} + y \frac{\partial y}{\partial q^j} \right) + \frac{F_v^{(l)}}{v} \left(\dot{x} \frac{\partial \dot{x}}{\partial \dot{q}^j} + \dot{y} \frac{\partial \dot{y}}{\partial \dot{q}^j} \right), \quad (3.11)$$

where we have used $\frac{\partial \mathbf{r}}{\partial q^j} = \frac{\partial \dot{\mathbf{r}}}{\partial \dot{q}^j}$. Considering (3.5) and the fact that the index j in the above equation takes values $j = r, \phi$, the radial and angular parts of the generalized force $Q_j^{(l)}$ above become (with $v = \sqrt{\dot{r}^2 + r^2 \dot{\phi}^2}$)

$$Q_r^{(l)} = F_r^{(l)} + \frac{F_v^{(l)} \dot{r}}{\left(\dot{r}^2 + r^2 \dot{\phi}^2 \right)^{\frac{1}{2}}}, \quad (3.12)$$

and

$$Q_\phi^{(l)} = \frac{F_v^{(l)} r^2 \dot{\phi}}{\left(\dot{r}^2 + r^2 \dot{\phi}^2 \right)^{\frac{1}{2}}}. \quad (3.13)$$

On the other hand, if we do not know the force itself but know the corresponding dissipative power $P^{(l)}$, we can write, using (3.10),

$$P^{(l)} = \frac{dE^{(l)}}{dt} = \mathbf{F}^{(l)} \cdot \mathbf{v} = F_r^{(l)} \dot{r} + F_v^{(l)} \left(\dot{r}^2 + r^2 \dot{\phi}^2 \right)^{\frac{1}{2}}. \quad (3.14)$$

where we have used the polar coordinates expressions $\mathbf{v} = \dot{r} \hat{\mathbf{r}} + r \dot{\phi} \hat{\boldsymbol{\phi}}$ and $\mathbf{r} = r \hat{\mathbf{r}}$. In cases where the force is (anti)parallel to \mathbf{v} , i.e., when $F_r^{(l)} = 0$, we obtain

$$F_v^{(l)} = \frac{P^{(l)}}{\left(\dot{r}^2 + r^2 \dot{\phi}^2 \right)^{\frac{1}{2}}}, \quad (3.15)$$

and (3.12) and (3.13) reduce to

$$Q_r^{(l)} = \frac{P^{(l)} \dot{r}}{\dot{r}^2 + r^2 \dot{\phi}^2}, \quad (3.16)$$

$$Q_\phi^{(l)} = \frac{P^{(l)} r^2 \dot{\phi}}{\dot{r}^2 + r^2 \dot{\phi}^2}. \quad (3.17)$$

C. Specific form of generalized forces

The generalized forces we consider in our model correspond to the first order PN correction $Q_j^{(1\text{PN})}$, the gravitational wave emission, which is also equal to the 2.5 order PN

correction $Q_j^{(\text{GW})} = Q_j^{(2.5\text{PN})}$, and the DM dynamical friction $Q_j^{(\text{DF})}$. In all of these expressions $j = r, \phi$. These corrective PN terms correspond to the leading orders for both orbital evolution; with the introduction of precession with the $Q_j^{(1\text{PN})}$ term, and GW emission term from $Q_j^{(2.5\text{PN})}$.

1. Post-Newtonian corrections and gravitational waves term

PN corrections to the relative acceleration of the two bodies can be written perturbatively as [32]

$$\frac{d\mathbf{v}}{dt} = \frac{Gm}{r^2} \left\{ \frac{1}{c^2} \mathbf{A}_{1\text{PN}} + \frac{1}{c^4} \mathbf{A}_{2\text{PN}} + \frac{1}{c^5} \mathbf{A}_{2.5\text{PN}} + \frac{1}{c^6} \mathbf{A}_{3\text{PN}} + \frac{1}{c^7} \mathbf{A}_{3.5\text{PN}} + \dots \right\}, \quad (3.18)$$

with c being the speed of light in vacuum. The first order term is of the form [32]

$$\mathbf{A}_{1\text{PN}} = \left\{ (4 + 2\eta) \frac{Gm}{r} - (1 + 3\eta)v^2 + \frac{3}{2}\eta\dot{r}^2 \right\} \hat{\mathbf{r}} + (4 - 2\eta)\dot{r}v\hat{\mathbf{v}}, \quad (3.19)$$

where $\eta = \mu/m$. Assuming the masses are time-independent, we have for the 1PN part of the force

$$\begin{aligned} \mathbf{F}^{(1\text{PN})} &= \mu \left. \frac{d\mathbf{v}}{dt} \right|_{1\text{PN}} \\ &= \frac{Gm\mu}{r^2 c^2} \left[(4 + 2\eta) \frac{Gm}{r} - (1 + 3\eta)v^2 + \frac{3}{2}\eta\dot{r}^2 \right] \hat{\mathbf{r}} + \frac{Gm\mu}{r^2 c^2} (4 - 2\eta)\dot{r}v\hat{\mathbf{v}}. \end{aligned} \quad (3.20)$$

As mentioned before, this is a velocity-dependent force, and hence it is best if we add it to our model as a generalized force. Replacing (3.20) into (3.12) we obtain

$$Q_r^{(1\text{PN})} = \frac{Gm\mu}{r^2 c^2} \left[(4 + 2\eta) \frac{Gm}{r} - (3\eta + 1)r^2 \dot{\phi}^2 + \dot{r}^2 \left(-\frac{7}{2}\eta + 3 \right) \right]. \quad (3.21)$$

Likewise, from (3.20) and (3.13) we get

$$Q_\phi^{(1\text{PN})} = (4 - 2\eta) \frac{Gm\mu}{c^2} \dot{r}\dot{\phi}. \quad (3.22)$$

The other PN correction we are considering is the $\mathbf{A}_{2.5\text{PN}}$ term which is the equivalent of the generalized force due to radiation of the gravitational waves away from the system. For this term we have [32]

$$\mathbf{A}_{2.5\text{PN}} = -\frac{8}{15}\eta \frac{Gm}{r} \left\{ \left(9v^2 + 17\frac{Gm}{r} \right) \dot{r}\hat{\mathbf{r}} - \left(3v^3 + 9\frac{Gm}{r}v \right) \hat{\mathbf{v}} \right\}, \quad (3.23)$$

which results in

$$\begin{aligned} \mathbf{F}^{(2.5\text{PN})} &= \mu \left. \frac{d\mathbf{v}}{dt} \right|_{2.5\text{PN}} \\ &= -\frac{8}{15}\eta \frac{G^2 m \mu}{r^3 c^5} \left[\left(9v^2 + 17\frac{Gm}{r} \right) \dot{r}\hat{\mathbf{r}} - \left(3v^3 + 9\frac{Gm}{r}v \right) \hat{\mathbf{v}} \right]. \end{aligned} \quad (3.24)$$

Using the above in (3.12), yields the radial part of the generalized force as

$$Q_r^{(2.5\text{PN})} = -\frac{8}{15}\eta\frac{G^2m^2\mu}{r^3c^5}\dot{r}\left[6\left(\dot{r}^2+r^2\dot{\phi}^2\right)+8\frac{Gm}{r}\right]. \quad (3.25)$$

In the same way, using (3.13), the angular order 2.5 generalized force becomes

$$Q_\phi^{(2.5\text{PN})} = \frac{8}{15}\eta\frac{G^2m^2\mu}{rc^5}\dot{\phi}\left(3\left(\dot{r}^2+r^2\dot{\phi}^2\right)+9\frac{Gm}{r}\right). \quad (3.26)$$

2. Dissipation due to dynamical friction

The gravitational interaction between m_2 and its local dark matter surrounding creates an effect similar in result to the force of friction and slows down the rotating object, even though no electromagnetic or other forces besides gravity are involved. This induces a dissipation of energy from the system, known as dynamical friction (DF). Its instantaneous power loss can be modeled as [17]

$$P^{(\text{DF})} = \frac{dE^{(\text{DF})}}{dt} = -4\pi G^2\frac{m_2^2\rho_{\text{DM}}(r)}{v}\xi(v)\ln(\Lambda). \quad (3.27)$$

Here, $\rho_{\text{DM}}(r)$ is the dark matter density profile, v is the relative speed of the objects where $v^2 = \dot{r}^2 + r^2\dot{\phi}^2$ in polar coordinates, and $\xi(v) = \gamma^2(1+v^2/c^2)^2$ is a relativistic correction to the DF in which $\gamma = \sqrt{1-v^2/c^2}$ is the familiar special relativistic factor. The term $(1+v^2/c^2)^2$ accounts for an increase in the deflection angle of the DM when considered as a collisional fluid due to the orbiting compact object, and γ^2 accounts for the relativistic momentum as seen by the compact object [33]. Furthermore, Λ is called the Coulomb logarithm and is defined as $\Lambda = b_{\text{max}}v_{\text{typ}}^2/G\mu$, where b_{max} is the maximum impact parameter and v_{typ}^2 is the typical speed (squared) of the rotating object (or the relative speed squared in the CM frame). We take $\Lambda = 3$ [17].

Since this force is assumed to act only parallel to \mathbf{v} , we can use the above formula in (3.16) and (3.17) to get⁶

$$Q_r^{(\text{DF})} = \frac{P^{(\text{DF})}\dot{r}}{\dot{r}^2+r^2\dot{\phi}^2} = -4\pi G^2m_2^2\xi(v)\rho_{\text{DM}}(r)\frac{\dot{r}}{\left(\dot{r}^2+r^2\dot{\phi}^2\right)^{\frac{3}{2}}}\ln(\Lambda), \quad (3.28)$$

$$Q_\phi^{(\text{DF})} = \frac{P^{(\text{DF})}r^2\dot{\phi}}{\dot{r}^2+r^2\dot{\phi}^2} = -4\pi G^2m_2^2\xi(v)\rho_{\text{DM}}(r)\frac{r^2\dot{\phi}}{\left(\dot{r}^2+r^2\dot{\phi}^2\right)^{\frac{3}{2}}}\ln(\Lambda). \quad (3.29)$$

⁶ Note that when $m_2 \ll m_1$, $\mu \approx m_2$.

D. Lagrangian equations of motion

We now have all the information to write down the Lagrangian equations of motion (3.6) and (3.7), which take the form

$$\frac{d}{dt} \left(\frac{\partial L}{\partial \dot{r}} \right) - \frac{\partial L}{\partial r} = Q_r^{(2.5\text{PN})} + Q_r^{(\text{DF})} + Q_r^{(1\text{PN})}, \quad (3.30)$$

$$\frac{d}{dt} \left(\frac{\partial L}{\partial \dot{\phi}} \right) - \frac{\partial L}{\partial \phi} = Q_\phi^{(2.5\text{PN})} + Q_\phi^{(\text{DF})} + Q_\phi^{(1\text{PN})}. \quad (3.31)$$

Replacing (3.8), (3.9), (3.21), (3.22), (3.25), (3.26), (3.28), and (3.29) in the above yields

$$\begin{aligned} \ddot{r} - r\dot{\phi}^2 + \frac{Gm}{r^2} = & -\frac{Gm}{c^2 r^2} \left[\frac{16G\mu\dot{r}}{5c^3 r} + 3\eta + 1 \right] \left(\dot{r}^2 + r^2 \dot{\phi}^2 \right) \\ & - \frac{G\dot{r}}{c^2 r^2} \left(\frac{64G^2 \mu m^2}{15c^3 r^2} - 4m\dot{r} + \frac{\mu\dot{r}}{2} \right) + \frac{2G^2 m}{c^2 r^3} (2m + \mu) \\ & - \frac{4\pi G^2 m_2^2 \xi \rho_{\text{DM}} \ln(\Lambda) \dot{r}}{\mu \left(\dot{r}^2 + r^2 \dot{\phi}^2 \right)^{3/2}}, \end{aligned} \quad (3.32)$$

and

$$\begin{aligned} r^2 \ddot{\phi} + 2r\dot{r}\dot{\phi} = & + \frac{8G^2 \mu m \dot{\phi}}{5c^5 r} \left(\dot{r}^2 + r^2 \dot{\phi}^2 \right) + \frac{2G\dot{r}\dot{\phi}}{c^2} (2m - \mu) \\ & + \frac{24G^3 \mu m^2 \dot{\phi}}{5c^5 r^2} - \frac{4\pi G^2 m_2^2 \xi \rho_{\text{DM}} \ln(\Lambda) r^2 \dot{\phi}}{\mu \left(\dot{r}^2 + r^2 \dot{\phi}^2 \right)^{3/2}} \end{aligned} \quad (3.33)$$

These coupled differential equations can be solved together numerically to yield the orbits.

IV. ORBITS AND GRAVITATIONAL WAVES

A. Orbital Evolution

For our given parameters, to illustrate the effect of these PN corrections and DM friction, the semi-major axis $a(t)$ was computed with the numerical solutions to (3.32) and (3.33) as an evolution measure for all the effects introduced into the Lagrangian. These can be found in Fig. 1.

As expected, DM friction accelerates the inspiral by several orders of magnitude. Note, however, that in the presence of DM, the addition of the 1PN term into the Lagrangian introduces another energy dissipation mechanism, which ultimately also accelerates orbital decay. This is particularly important during the later stages of the inspiral, where it differs from the regular GW radiative term. Note that the oscillations in the semi-major axis due to orbital precession from the 1PN term are still present at the later stages of the evolution, it is simply the scaling to plot it alongside its no-1PN-corrections counterpart that the oscillations appear to vanish.

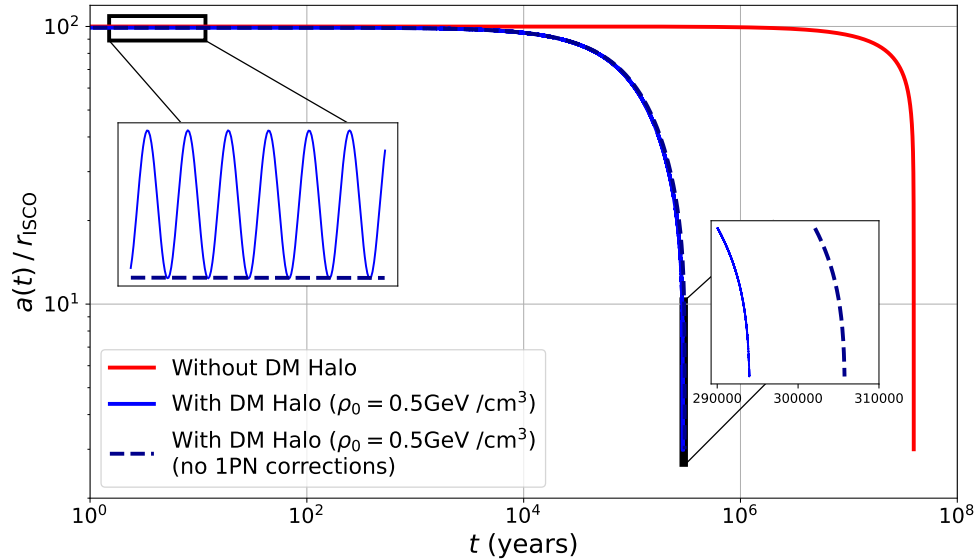


Figure 1. Semi-major axis of the orbit as a function of time, where in all cases evolution ranges from $100 r_{\text{ISCO}}$ to $3 r_{\text{ISCO}}$. The dynamical friction term expedites energy dissipation and modifies the radial evolution of the binary. The no 1PN corrections curve refers to setting the $Q_j^{(1\text{PN})}$ terms to zero, which has a noticeable effect, especially at the latter stages of the inspiral. All the curves above include the GW dissipative term.

B. Gravitational Wave Analysis

Gravitational wave observatories measure the strain of the waves, which is the Fourier mode h_σ of the perturbations h_{ij} , where $\sigma = +, \times$ are the polarization of the waves. Having found the orbits by solving the equations of motions (3.32) and (3.33), we replace the resulting $r(t)$ and $\phi(t)$ in

$$x(t) = r(t) \cos[\phi(t)], \quad (4.1)$$

$$y(t) = r(t) \sin[\phi(t)], \quad (4.2)$$

and use the Cartesian Dirac deltas to express the matter density of the system as

$$\rho(\mathbf{x}, t) = \rho_{\text{DM}}(r) + \mu \delta(x - x(t)) \delta(y - y(t)) \delta(z). \quad (4.3)$$

Using these, we can find the quadrupole moment tensor

$$M^{ij} = \int x^i x^j \rho(t, \mathbf{x}) d^3x, \quad (4.4)$$

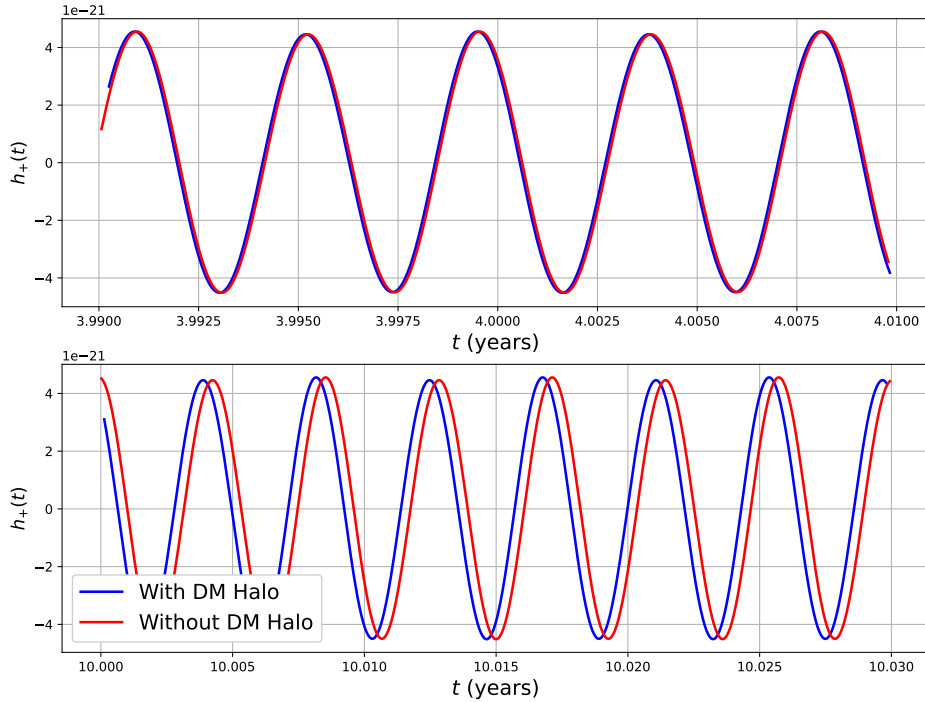


Figure 2. Example of the time-domain “plus” polarization waveform, $h_+(t)$, following the evolution of the $\rho_0 = 0.5 \text{ GeV/cm}^3$ DM halo vs. vacuum with all PN corrections. Assuming the system enters in-band at the early stages of the inspiral ($70 r_{\text{ISCO}}$ at $t = 0$), and at a point where the DM mini-spike is not at its densest, the timescale of this dephasing is set to start at about the four-year mark, which is given by LISA’s lifetime.

where $i, j = 1, 2, 3$ correspond to x, y, z coordinates respectively. Finally, we can use M^{ij} to compute the plus and cross polarizations of the gravitational wave strains using

$$\begin{aligned}
 h_+(t; \bar{\theta}, \bar{\phi}) = \frac{1}{R} \frac{G}{c^4} & \left[\ddot{M}_{11} (\cos^2(\bar{\phi}) - \sin^2(\bar{\phi}) \cos^2(\bar{\theta})) \right. \\
 & + \ddot{M}_{22} (\sin^2(\bar{\phi}) - \cos^2(\bar{\phi}) \cos^2(\bar{\theta})) \\
 & - \ddot{M}_{33} \sin^2(\bar{\theta}) - \ddot{M}_{12} \sin(2\bar{\phi}) (1 + \cos^2(\bar{\theta})) \\
 & \left. + \ddot{M}_{13} \sin(\bar{\phi}) \sin(2\bar{\theta}) + \ddot{M}_{23} \cos(\bar{\phi}) \sin(2\bar{\theta}) \right] \quad (4.5)
 \end{aligned}$$

and

$$\begin{aligned}
 h_\times(t; \bar{\theta}, \bar{\phi}) = \frac{1}{R} \frac{G}{c^4} & \left[(\ddot{M}_{11} - \ddot{M}_{22}) \sin(2\bar{\phi}) \cos(\bar{\theta}) \right. \\
 & + 2\ddot{M}_{12} \cos(2\bar{\phi}) \cos(\bar{\theta}) - 2\ddot{M}_{13} \cos(2\bar{\phi}) \sin(\bar{\theta}) \\
 & \left. + 2\ddot{M}_{23} \sin(2\bar{\phi}) \sin(\bar{\theta}) \right], \quad (4.6)
 \end{aligned}$$

where R is the distance of the observatory to the CM of the binary system, and $\bar{\theta}, \bar{\phi}$ are related to the relative orientation of the frames of reference of the source and the observer

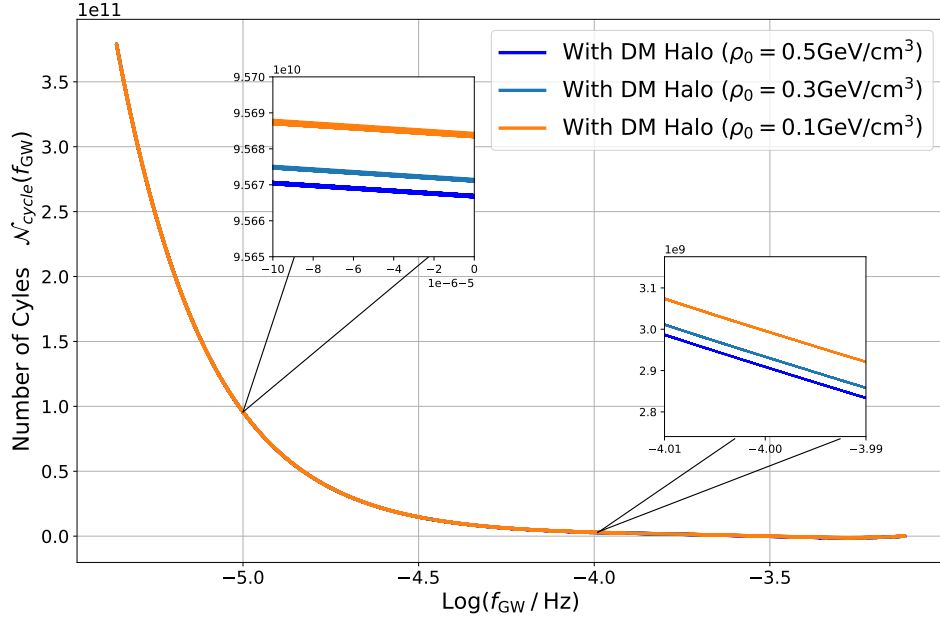


Figure 3. Number of cycles comparison for different DM densities and vacuum as a function of GW frequency. Inset plots represent zoomed-in sections of the main plot at 10^{-5} Hz (left inset) and 10^{-4} Hz (right inset).

[34]. A benefit to this approach is that by directly solving the Lagrangian equations of motion, one can freely compute the explicit waveforms as a function of time, where we can observe the rapid effect from DM friction through the dephasing of the waveforms. For our purposes we have considered a source at $\{R, \bar{\theta}, \bar{\phi}\} = \{1\text{Mpc}, 0, 0\}$. Note that with this choice of angles $h(t) = h_+(t)$. The result is plotted in Fig. 2.

To fully encapsulate this GW dephasing effect, we analyze the number of cycles, $\mathcal{N}_{\text{cycle}}$, that the system can be in-band as a function of the gravitational wave frequency, f_{GW} . Note that for this, one may use the relations that come directly from solving the Lagrangian equations of motion of the phase $\phi(t)$, which is related to the GW phase with $\phi_{GW}(t) = 2\phi(t)$, and the number of cycles would simply be

$$\mathcal{N}_{\text{cycle}}(t) \equiv \frac{\phi_{\text{No DM}}(t) - \phi_{\text{DM}}(t)}{\pi} \quad (4.7)$$

Accompanying by the following relation

$$\dot{\phi}(t) = 2\pi f_{GW}(t), \quad (4.8)$$

one may obtain $\mathcal{N}_{\text{cycle}}(f_{GW})$ with the help of the solutions to (3.32) and (3.33). One can see the result in Fig. 3.

The number of cycles in the presence of a DM halo will be lower than in a vacuum, which is expected as the DM friction would translate a faster inspiral into fewer orbits being in-band for GW emission. What is important for the detection of a DM spike from DM friction would be the particular shape of the waveform in frequency space, as interferometers set out to find

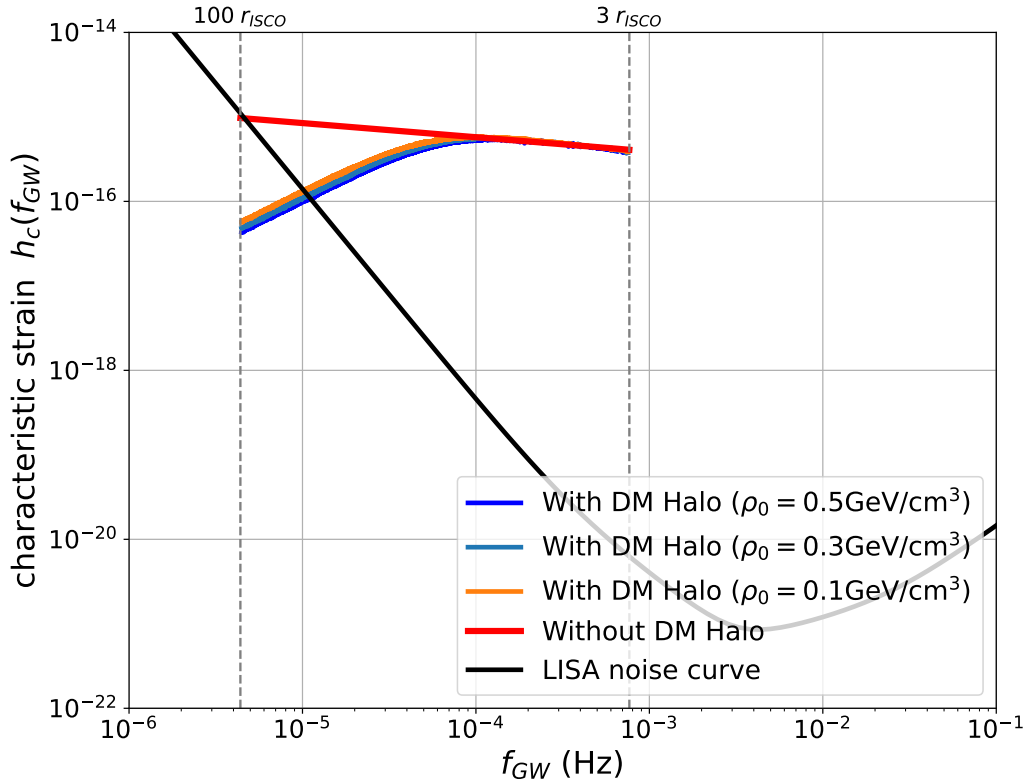


Figure 4. The strain and detectability for LISA’s sensitivity curve given for various DM densities parametrized by ρ_0 . GW energy dissipation is dominant over DM friction during the later stages of the inspiral, which can be seen by the agreement of all strains at higher frequencies. Thus, searches for this DM friction would be the most sensitive during earlier parts of the inspiral, but not earlier than the strain curves crossing LISA’s sensitivity. For our choice of parameters, this occurs near 10^{-5} Hz.

signals from match-filtering techniques in the spectral domain. Hence, it is more illustrative to work in the frequency domain. In particular, we are interested in the detectability of these results with the LISA sensitivity curve, as well as the different signatures obtained from changing DM parameters. To adequately compare this to the detector’s sensitivity to estimate signal-to-noise ratios, we compute the characteristic strain $h_c(f_{GW})$ given by

$$h_c(f_{GW}) = 2f_{GW}|\tilde{h}(f_{GW})| \quad (4.9)$$

with $\tilde{h}(f_{GW})$ being the Fourier transform of the GW time signal. The numerical computation of the frequency domain in the case of the system we chose compared to the LISA sensitivity curve can be seen in Fig. 4. One can see there is a clear distinction between the cases with DM halo and the case without DM halo in lower frequencies which will be observable by LISA.

V. DISCUSSION AND CONCLUSION

Compact binary systems with an environment around them, particularly a DM spike, are a valuable experimental arena for the potential detection of effects associated with new physics, particularly the detection of the effects of DM on the emitted gravitational wave from such systems. Therefore, it is important to have a robust theoretical framework that can incorporate as many physical effects as possible, particularly general relativistic and DM effects. In this paper, we have presented a powerful yet rather simple Lagrangian formalism that allows the incorporation of these effects, in particular post-Newtonian corrections to the orbit up to any desired order, as well as dynamical friction from DM. This allows us to expand the range of validity of the orbital evolution throughout the later stages of the inspiral. In addition to presenting this framework, we have also employed it in the case where in addition to dynamical friction, we have considered the most important PN corrections, i.e., 1PN and 2.5PN, corresponding to the orbital precession and gravitational wave dissipation respectively. After obtaining the analytical Lagrangian equations of motion, we have solved them numerically to obtain the orbits. We have then used these solutions to compare the orbits in cases with and without DM halo and PN corrections. Furthermore, using the orbit equations, we have derived the modified GW waveform emitted from the binary in the presence of a DM spike, which shows a dephasing effect compared to the no-DM case. Moreover, we have also computed the frequency space strain of the GWs for three different DM densities and compared them against the LISA frequency sensitivity curve. Our calculations show that the modification effects resulting from the presence of DM spike are observable by LISA.

As mentioned before, due to the power of our proposed Lagrangian framework, one can include post-Newtonian corrections up to any order and in particular, corrections to both the orbital motion and GW emission up to the recently derived higher order terms [35]. Therefore, our framework could be quite beneficial in the search for DM effects since following a potential inspiral beyond the Newtonian regime of the evolution will provide better GW templates for match filtering methods with the LISA detector or other observatories such as Cosmic Explorer. One may also imagine modifying the Lagrangian to add other effects such as accretion of DM by the binary, which can be incorporated into our framework quite easily. Lastly, our framework also provides the liberty to modify the environment density $\rho(r)$ to include dynamical and companion interaction effects $\rho(r) \rightarrow \rho(t, r, \phi)$.

ACKNOWLEDGMENTS

We thank Gianfranco Bertone for valuable discussions and input. This work has emerged as a follow-up from the international innovative teaching and research program EXPLORE (“EXPeriential Learning Opportunity through Research and Exchange”) of York University, the University of Alberta, and Goethe University Frankfurt. We thank all mentors, junior mentors and participants of EXPLORE for stimulating discussions and a fruitful collaboration. The EXPLORE program is supported by the Academic Innovation Fund (AIF) at York University, Goethe University QSL (“Quality Assurance in Teaching”) funds, the State of Hesse within the Research Cluster ELEMENTS (Project ID 500/10.006), and the Deutsche Forschungsgemeinschaft (DFG, German Research Foundation) through the CRC-TR 211 “Strong-interaction matter under extreme conditions”– project number 315477589-TRR 211. S. R. acknowledges the support of the Natural Science and Engineering Research Council of

Canada, funding reference No. RGPIN-2021-03644 and No. DGEER-2021-00302.

Appendix A: Analytical approximation of the characteristic strain

One may attempt to compute the strain $h_c(f)$ directly using the stationary phase approximation (SPA)

$$\tilde{h}_{+,\times}(f) = \int h_{+,\times}(t) e^{2\pi i f t} dt \approx \frac{1}{2} A_{+,\times}(f) e^{i\Psi_{+,\times}(f)}, \quad (\text{A1})$$

where

$$A_+(f) = A_0(f) \left(\frac{1 + \cos^2(\bar{\theta})}{2} \right), \quad A_\times(f) = A_0(f) \left(\cos(\bar{\theta}) \right), \quad (\text{A2})$$

and

$$A_0(f) = \frac{4 (GM)^{5/3} (\pi f)^{2/3}}{R c^4} \left(\frac{2\pi}{\ddot{\phi}(f)} \right)^{1/2}, \quad (\text{A3})$$

and

$$\Psi_+(f) = 2\pi f t_c - \phi_c - \frac{\pi}{4} + \phi(f), \quad \Psi_\times(f) = \Psi_+(f) + \frac{\pi}{2}. \quad (\text{A4})$$

Here t_c and ϕ_c are time and phase at coalescence, respectively. We should note that solving (3.32) and (3.33) in time will provide us with $\phi(t)$ to insert in both (A2) and (A4). This can be related to the frequency domain with the time, frequency and orbital phase relation

$$\dot{\phi}(t) = 2\pi f(t). \quad (\text{A5})$$

This approach, however, is not immediately useful as $\ddot{\phi}(f)$ will be an oscillatory function of f , which can take negative values due to the introduction of precession from the 1PN term. Hence, the complete Fourier transform has to be computed numerically.

-
- [1] B. P. Abbott *et al.* (LIGO Scientific, Virgo), *Phys. Rev. Lett.* **116**, 221101 (2016), [Erratum: *Phys. Rev. Lett.* 121, no.12, 129902(2018)], [arXiv:1602.03841 \[gr-qc\]](#).
 - [2] P. Amaro-Seoane *et al.* (LISA), (2017), [arXiv:1702.00786 \[astro-ph.IM\]](#).
 - [3] W.-R. Hu and Y.-L. Wu, *National Science Review* **4**, 685 (2017).
 - [4] J. Luo *et al.* (TianQin), *Class. Quant. Grav.* **33**, 035010 (2016), [arXiv:1512.02076 \[astro-ph.IM\]](#).
 - [5] K. G. Arun *et al.* (LISA), *Living Rev. Rel.* **25**, 4 (2022), [arXiv:2205.01597 \[gr-qc\]](#).
 - [6] P. Auclair *et al.* (LISA Cosmology Working Group), *Living Rev. Rel.* **26**, 5 (2023), [arXiv:2204.05434 \[astro-ph.CO\]](#).
 - [7] A. Addazi *et al.*, *Prog. Part. Nucl. Phys.* **125**, 103948 (2022), [arXiv:2111.05659 \[hep-ph\]](#).
 - [8] R. Alves Batista *et al.*, (2023), [arXiv:2312.00409 \[gr-qc\]](#).
 - [9] A. Garcia-Chung, M. F. Carney, J. B. Mertens, A. Parvizi, S. Rastgoo, and Y. Tavakoli, (2023), [arXiv:2305.18192 \[gr-qc\]](#).
 - [10] A. Garcia-Chung, M. F. Carney, J. B. Mertens, A. Parvizi, S. Rastgoo, and Y. Tavakoli, *JCAP* **11**, 054, [arXiv:2208.09739 \[gr-qc\]](#).

- [11] A. Garcia-Chung, J. B. Mertens, S. Rastgoo, Y. Tavakoli, and P. Vargas Moniz, *Phys. Rev. D* **103**, 084053 (2021), [arXiv:2012.09366 \[gr-qc\]](#).
- [12] G. Bertone, D. Hooper, and J. Silk, *Phys. Rept.* **405**, 279 (2005), [arXiv:hep-ph/0404175](#).
- [13] G. Bertone and T. Tait, M. P., *Nature* **562**, 51 (2018), [arXiv:1810.01668 \[astro-ph.CO\]](#).
- [14] P. Gondolo and J. Silk, *Phys. Rev. Lett.* **83**, 1719 (1999), [arXiv:astro-ph/9906391](#).
- [15] L. Sadeghian, F. Ferrer, and C. M. Will, *Phys. Rev. D* **88**, 063522 (2013), [arXiv:1305.2619 \[astro-ph.GA\]](#).
- [16] K. Eda, Y. Itoh, S. Kuroyanagi, and J. Silk, *Phys. Rev. Lett.* **110**, 221101 (2013), [arXiv:1301.5971 \[gr-qc\]](#).
- [17] K. Eda, Y. Itoh, S. Kuroyanagi, and J. Silk, *Phys. Rev. D* **91**, 044045 (2015), [arXiv:1408.3534 \[gr-qc\]](#).
- [18] A. Barrau, M. Bojowald, G. Calcagni, J. Grain, and M. Kagan, *JCAP* **05**, 051, [arXiv:1404.1018 \[gr-qc\]](#).
- [19] A. Coogan, G. Bertone, D. Gaggero, B. J. Kavanagh, and D. A. Nichols, (2021), [arXiv:2108.04154 \[gr-qc\]](#).
- [20] C. F. B. Macedo, P. Pani, V. Cardoso, and L. C. B. Crispino, *Astrophys. J.* **774**, 48 (2013), [arXiv:1302.2646 \[gr-qc\]](#).
- [21] X.-J. Yue and W.-B. Han, *Phys. Rev. D* **97**, 064003 (2018), [arXiv:1711.09706 \[gr-qc\]](#).
- [22] X.-J. Yue and Z. Cao, *Phys. Rev. D* **100**, 043013 (2019), [arXiv:1908.10241 \[astro-ph.HE\]](#).
- [23] V. Cardoso, C. F. B. Macedo, and R. Vicente, *Phys. Rev. D* **103**, 023015 (2021), [arXiv:2010.15151 \[gr-qc\]](#).
- [24] N. Becker, L. Sagunski, L. Prinz, and S. Rastgoo, *Phys. Rev. D* **105**, 063029 (2022), [arXiv:2112.09586 \[gr-qc\]](#).
- [25] N. Becker and L. Sagunski, *Phys. Rev. D* **107**, 083003 (2023), [arXiv:2211.05145 \[gr-qc\]](#).
- [26] N. Dai, Y. Gong, T. Jiang, and D. Liang, (2021), [arXiv:2111.13514 \[gr-qc\]](#).
- [27] B. J. Kavanagh, D. A. Nichols, G. Bertone, and D. Gaggero, *Phys. Rev. D* **102**, 083006 (2020), [arXiv:2002.12811 \[gr-qc\]](#).
- [28] N. Speeney, A. Antonelli, V. Baibhav, and E. Berti, *Phys. Rev. D* **106**, 044027 (2022), [arXiv:2204.12508 \[gr-qc\]](#).
- [29] P. S. Cole, A. Coogan, B. J. Kavanagh, and G. Bertone, (2022), [arXiv:2207.07576 \[astro-ph.CO\]](#).
- [30] K. A. Arnaud *et al.*, *AIP Conf. Proc.* **873**, 619 (2006), [arXiv:gr-qc/0609105](#).
- [31] J. F. Navarro, C. S. Frenk, and S. D. M. White, *The Astrophysical Journal* **490**, 493 (1997).
- [32] C. M. Will, *Proc. Nat. Acad. Sci.* **108**, 5938 (2011), [arXiv:1102.5192 \[gr-qc\]](#).
- [33] D. Traykova, K. Clough, T. Helfer, E. Berti, P. G. Ferreira, and L. Hui, *Phys. Rev. D* **104**, 103014 (2021), [arXiv:2106.08280 \[gr-qc\]](#).
- [34] M. Maggiore, *Gravitational Waves: Volume 1: Theory and Experiments* (Oxford University Press, Oxford, 2007).
- [35] L. Blanchet *et al.*, (2023), [arXiv:2304.13647](#).